ELSEVIER

Journal of Alloys and Compounds 330–332 (2002) 732–737

Journal of ALLOYS AND COMPOUNDS

www.elsevier.com/locate/jallcom

Hydrogen storage properties of amorphous and nanocrystalline Zr–Ni–V alloys

K. Tanaka[a,*], M. Sowa[a], Y. Kita[a], T. Kubota[b], N. Tanaka[b]

[a]*Department of Materials Science and Engineering, Nagoya Institute of Technology, Nagoya 466-8555, Japan*
[b]*Department of Applied Physics, Graduate School of Engineering, Nagoya University, Nagoya 464-8603, Japan*

Abstract

Hydrogen storage properties, such as hydrogen absorbency, hydriding–dehydriding kinetics, *P–C–T* characteristics and thermal desorption spectra, were studied for amorphous, nanocrystalline and as-cast crystalline phases of Zr–Ni–V alloys near the equiatomic composition. The nanocrystalline alloys were obtained from melt-spun amorphous ribbons by crystallizing at moderate temperatures. Their structures were examined by X-ray diffraction and transmission electron microscopy. The hydrogen storage properties of the nanocrystalline alloys were in general superior to the corresponding amorphous alloys but inferior to the as-cast alloys particularly in the dehydriding properties as revealed by thermal desorption spectra.

Keywords: Zr–Ni–V system; Amorphous alloy; Nanocrystalline alloy; *P–C–T* characteristics; Thermal desorption spectra; X-ray diffraction; TEM observation

1. Introduction

Ternary Zr–Ni–V alloys near the center of the composition triangle have a crystalline phase of cubic C15 or hexagonal C14 Laves structure, and their hydrogen storage properties have been studied by several researchers for battery electrode application [1–3]. These alloys are interesting from the viewpoints not only of practical applications but also of basic research because they can take amorphous as well as nanocrystalline structures when they are rapidly quenched from the melts and subsequently annealed above the crystallization temperature T_x. Specifically, the nanocrystalline alloys attract our attention since they may have hydrogen absorbency and hydriding–dehydriding (H–D) kinetics superior to ordinary crystalline phases of as-cast alloys [4]. The objective of this study is to reveal the hydrogen storage properties of these three kinds of alloys and relate them to the characteristic structures of the alloys.

*Corresponding author. Tel.: +81-52-735-5298; fax: +81-52-735-5316.

E-mail address: tanaka@mse.nitech.ac.jp (K. Tanaka).

2. Experimental

Amorphous $Zr_{35}Ni_{65-x}V_x$ ($x=10$ to 25) and $Zr_{25}Ni_{75-x}V_x$ ($x=10$ to 50) alloy ribbons (~1 mm wide and ~20 μm thick) were prepared with melt-spinning technique and subjected to annealing in vacuum of $\sim 8\times 10^{-5}$ Pa at temperatures above T_x~800 K to obtain nanocrystalline alloys. Their phases and microstructures were examined with X-ray diffraction (XRD) using Cu Kα radiation and transmission electron microscopy (TEM). The H–D kinetics and pressure–composition isotherms (*P–C–T*) of these melt-spun and crystallized alloys were measured at 423 K and compared with those of as-cast alloys. Thermal desorption spectra (TDS) were also measured to examine the desorption properties at higher temperatures. To promote the hydrogen absorption, the amorphous ribbons were cut into pieces of 2–3 mm in length; the nanocrystallized alloys were ground into powders of 70 mesh (≲200 μm); and the as-cast alloys were also ground into powders of 70 mesh and homogenized at 1073 K for 5 h in vacuum.

The XRD analyses of the as-cast alloys showed that $Zr_{35}Ni_{65-x}V_x$ consisted of C15 + $Ni_{10}Zr_7$ (for $x=10$) or C14 + NiZr ($x=25$), while $Zr_{25}Ni_{75-x}V_x$ consisted of C15 + Ni_3Zr ($x=10$), C15 ($x=25$, 35, 37.5), C15 + $Ni_{10}Zr_7$

0925-8388/02/$ – see front matter
PII: S0925-8388(01)01656-5

($x=40$) or C14+NiZr ($x=50$). In this paper, we mainly report the results on $Zr_{35}Ni_{55}V_{10}$ and $Zr_{25}Ni_{37.5}V_{37.5}$ (or occasionally $Zr_{25}Ni_{40}V_{35}$) alloys, which present different crystallization processes and have different equilibrium phase structure from each other.

3. Results and discussion

3.1. Crystallization behavior of amorphous alloys

Fig. 1 shows XRD patterns of amorphous $Zr_{35}Ni_{55}V_{10}$ alloy and ones subjected to annealing for 30 min at each indicated temperature, compared with that of as-cast alloy. In this alloy, $Ni_{10}Zr_7$ precipitates together with other unknown crystalline phases in the amorphous matrix above ~800 K, and they develop with increasing temperature up to 973 K. This structure is altered to $Ni_{10}Zr_7$+C15 mixed equilibrium phases at 1073 K, which is consistent with that of the as-cast alloy. The diffraction peaks of $Ni_{10}Zr_7$ and the unknown phases observed after annealing at 873 and 973 K are much broader than those of the as-cast alloy, suggesting that nanocrystalline phases are formed after annealing at these lower temperatures.

Fig. 2 shows a similar result on amorphous $Zr_{25}Ni_{40}V_{35}$ alloy. In this alloy the crystallization takes place at T_x~823 K, and above 873 K diffraction peaks attributable to a C14 Laves phase develop up to 1073 K, where the alloy consists only of the C14 phase. This phase is, however, considered to be nonequilibrium and is expected to alter to a C15 equilibrium phase after further annealing at this temperature, as evidenced by the as-cast alloy which has been annealed at 1073 K for 5 h. Since the diffraction peaks of the C14 phase of the samples annealed at 873–973 K are much broader than those of the sample annealed at 1073 K, nanocrystalline structures of the C14 phase are expected to be formed at 873–973 K. We have observed essentially the same crystallization behavior as above for amorphous $Zr_{25}Ni_{37.5}V_{37.5}$ alloy, as shown in Fig. 3, whereas, for amorphous $Zr_{25}Ni_{50}V_{25}$ alloy (not shown), the crystallization product was a C15 equilibrium phase instead of a C14 nonequilibrium one.

Fig. 4 shows TEM images and the corresponding electron diffraction patterns of a small fragment of amorphous $Zr_{25}Ni_{37.5}V_{37.5}$ alloy ribbon and the same sample

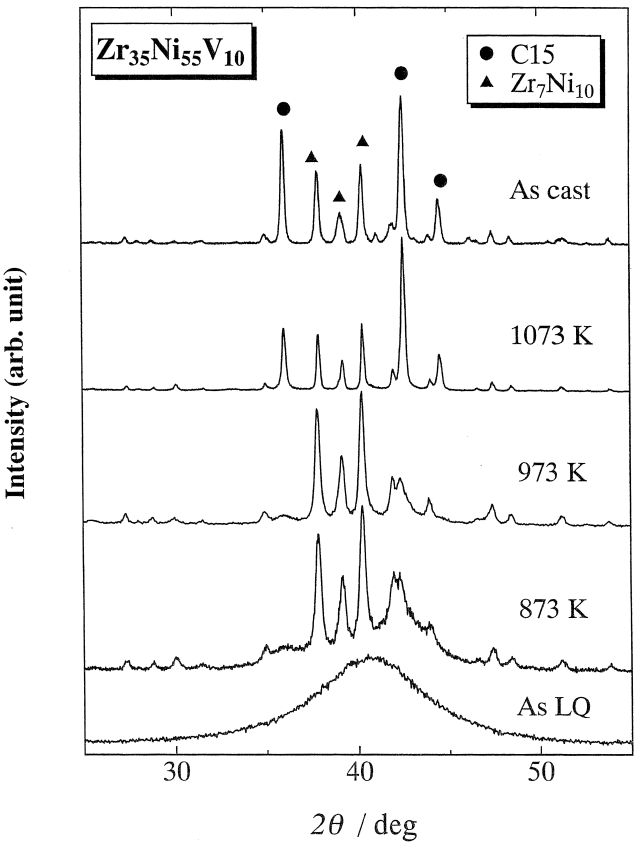

Fig. 1. XRD patterns of amorphous $Zr_{35}Ni_{55}V_{10}$ alloy and ones subjected to annealing for 30 min at each indicated temperature, compared with that of as-cast alloy.

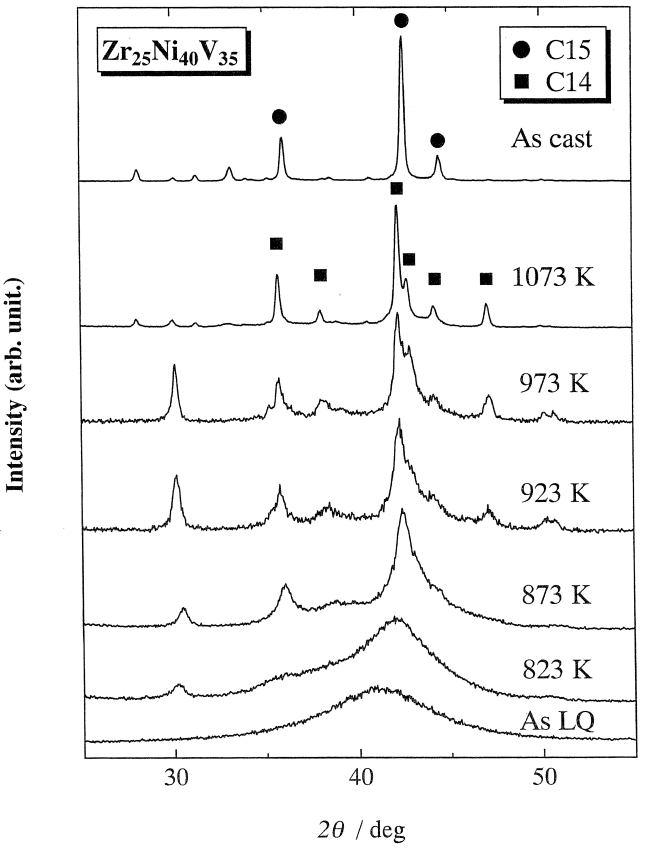

Fig. 2. XRD patterns of amorphous $Zr_{25}Ni_{40}V_{35}$ alloy and ones subjected to annealing for 30 min at indicated temperatures, compared with that of as-cast alloy.

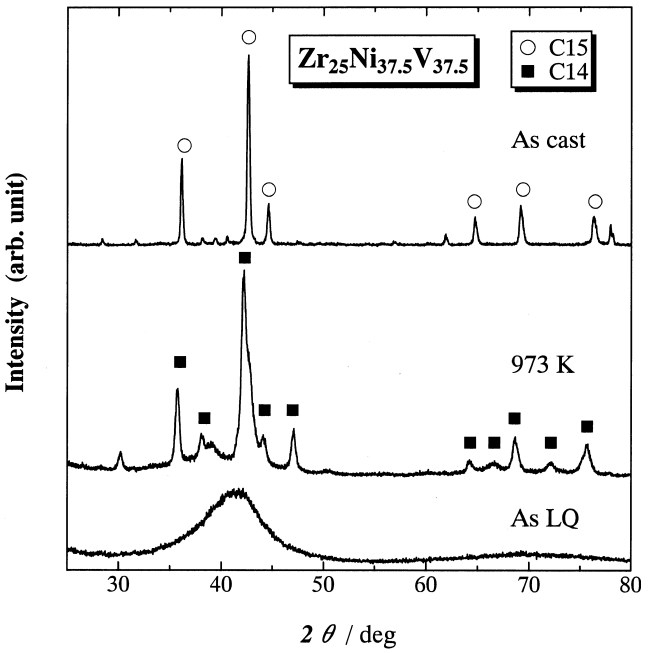

Fig. 3. XRD patterns of amorphous $Zr_{25}Ni_{37.5}V_{37.5}$ alloy and one subjected to annealing for 30 min at 973 K, compared with that of as-cast alloy.

continually heated in situ in the microscope. The temperature was raised stepwise from room temperature to successively higher temperatures in 20–40-min steps and held at each indicated temperature for 5 min for stabilization. It can be seen from this figure that nanocrystalline precipitates, smaller than ~5 nm in size, emerge in the amorphous matrix at 923 K and grow in size with increasing temperature. The sample is wholly filled with nanocrystalline grains of ~10 nm at 1129 K. This shows that the nanocrystalline structure is stable to ~1000 K.

3.2. Hydrogen storage properties

The amorphous, nanocrystalline and as-cast alloys of $Zr_{35}Ni_{55}V_{10}$ and $Zr_{25}Ni_{37.5}V_{37.5}$ thus prepared were hydrided under 2.8–3.0 MPa H_2 at 423 K for durations long enough to reach the equilibrium, and then dehydrided at 673 K for 3 h in vacuum. The dehydriding was complete for the as-cast alloy, but was not complete for the nanocrystalline and amorphous alloys because certain amounts of hydrogen were still left undesorbed at 673 K, as revealed by the TDS spectra shown later. This H–D treatment was repeated for10 cycles to achieve complete activation and stabilization of the samples. Fig. 5 shows the hydriding behavior of the three kinds of $Zr_{25}Ni_{37.5}V_{37.5}$ alloy, where the amount of absorbed hydrogen is plotted against holding time for the 1st to 10th cycle. It can be seen that the amorphous alloy is activated quite slowly, while the nanocrystalline (annealed at 973 K) and as-cast alloys are activated quickly. A similar behavior has been observed for $Zr_{35}Ni_{55}V_{10}$ alloy.

Fig. 6 shows the P–C–T characteristics at 423 K of the three kinds of $Zr_{25}Ni_{37.5}V_{37.5}$ alloy subjected to ten H–D cycles. In the amorphous alloy, the P–C–T curve rises up and falls down steeply without manifesting any plateau-like feature, while, in the nanocrystalline and as-cast alloys, the curves are much less sloped with a definite hysteresis; however, a plateau-like feature is not still observed. The maximum hydrogen contents of these samples at 3 MPa H_2 amount to $H/M = 0.60$ (amor.), 0.66 (nano.) and 0.80 (as-cast). The XRD patterns of the fully hydrided samples (not shown) shifted uniformly toward the lower angles without presenting new diffraction peaks, indicating that the hydrogen atoms were dissolved in these samples preserving the original amorphous, nanocrystalline (C14) and equilibrium crystalline (C15) structures. Therefore, it is expected that, in all these alloys, hydrogen is entirely stored in the form of solid solutions.

Fig. 7 shows P–C–T results for $Zr_{35}Ni_{55}V_{10}$ alloy, where the maximum hydrogen contents amount to $H/M =$ 0.40 (amor.), 0.55 (nano.) and 0.36 (as-cast). The decrease of the hydrogen content in the as-cast alloy, compared with the amorphous and nanocrystalline alloys, may be attributed to the two-phase structure of $Ni_{10}Zr_7$ + C15. The P–C–T features of these samples are similar to those of $Zr_{25}Ni_{37.5}V_{37.5}$ alloy except for the decrease in the maximum hydrogen contents.

3.3. Thermal desorption spectra

Fig. 8 shows TDS spectra of the three kinds of $Zr_{25}Ni_{37.5}V_{37.5}$ alloy loaded with the maximum amounts of hydrogen, where the samples were heated at a constant rate of 10 K min^{-1}. In the amorphous alloy, the desorption takes place in a temperature range centered around 650 K, while, in the nanocrystalline alloy, it occurs in a wider range centered around 550 K; in contrast, in the as-cast alloy, the desorption is completed in a narrow range around 400 K. These features of TDS reflect the degree of thermal stability of dissolved hydrogen in the samples [5]. It is obvious that the stability of hydrogen in the nanocrystalline alloy lies between the amorphous and the equilibrium crystalline alloys. A similar trend has been found in other alloy systems [6–8].

Fig. 9 shows similar results on $Zr_{35}Ni_{55}V_{10}$ alloy, where the TDS spectra of amorphous, nanocrystalline (crystallized at 873 and 973 K) and as-cast samples are compared. Here, the decrease in thermal stability of hydrogen from amorphous to nanocrystalline and to equilibrium crystalline phases is reconfirmed. The higher Zr content of this alloy compared with the previous one increases the hydrogen stability in the alloy and hence raises the desorption temperature of the amorphous alloy significantly.

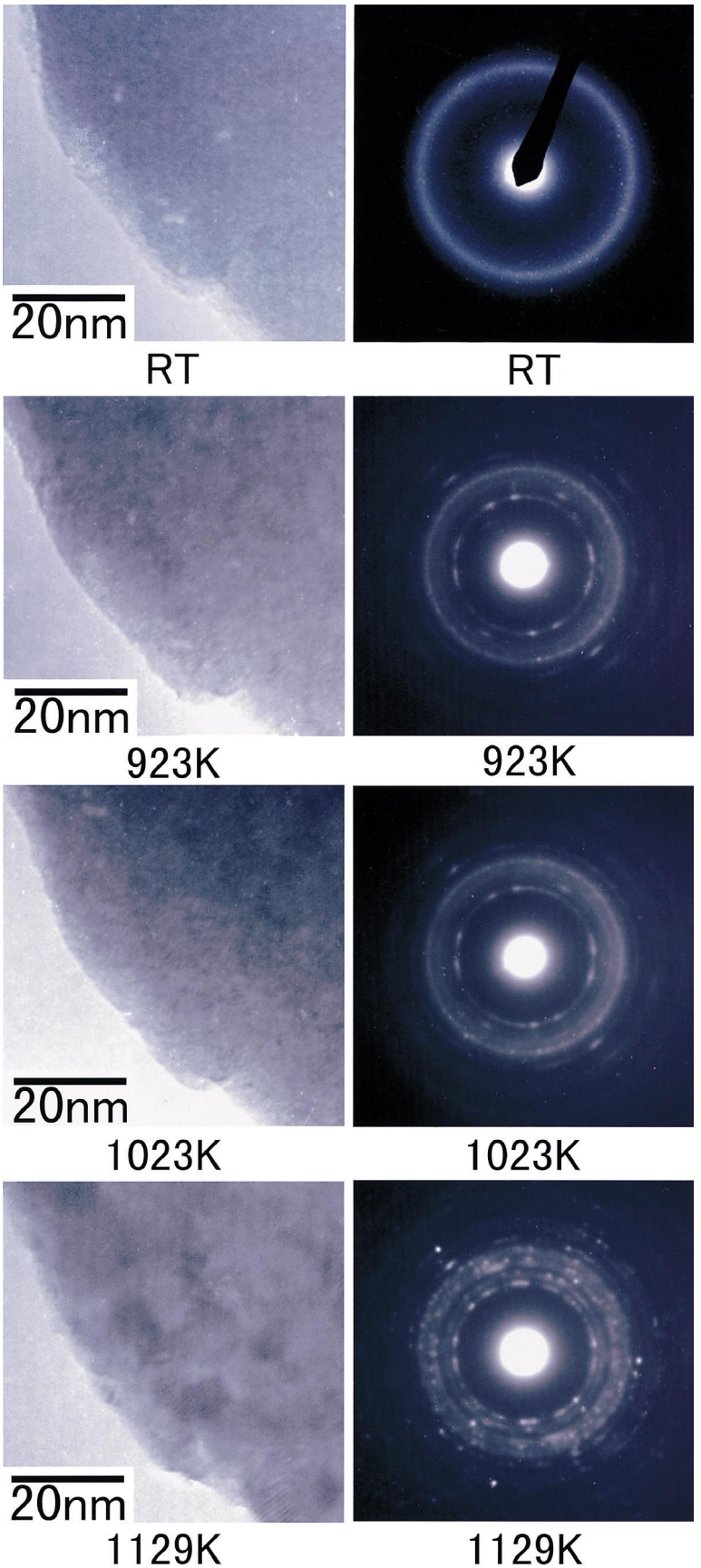

Fig. 4. TEM images and the corresponding ED patterns of amorphous $Zr_{25}Ni_{37.5}V_{37.5}$ alloy continually heated in situ in the microscope.

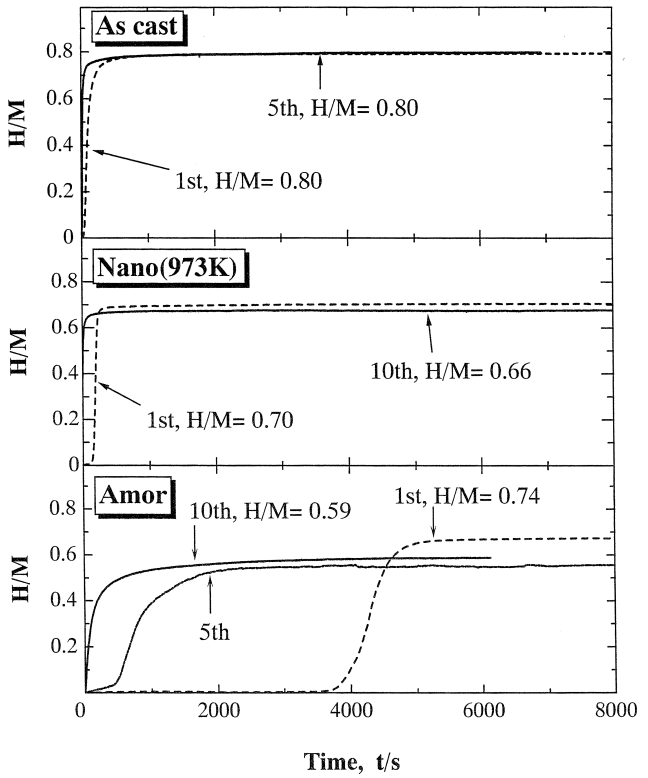

Fig. 5. Hydriding behavior of amorphous, nanocrystalline (crystallized at 973 K) and as-cast $Zr_{25}Ni_{37.5}V_{37.5}$ alloys under 30 MPa H_2 at 423 K.

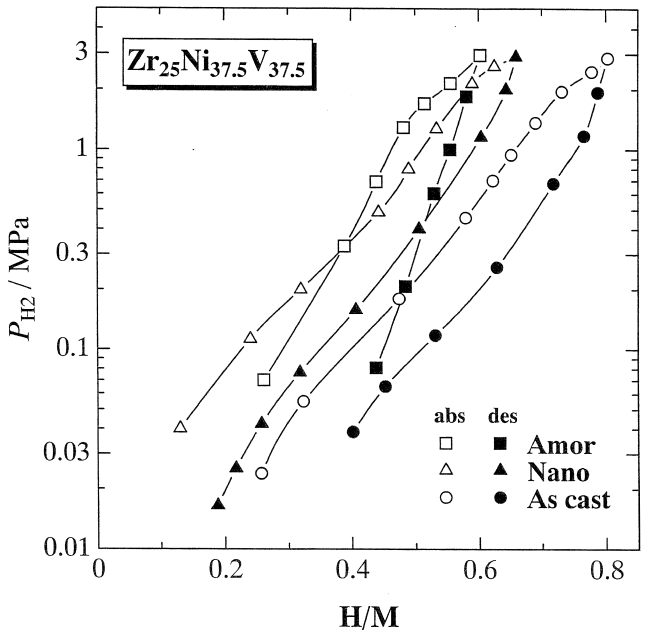

Fig. 6. *P–C–T* characteristics at 423 K of amorphous, nanocrystalline (crystallized at 973 K) and as-cast $Zr_{25}Ni_{37.5}V_{37.5}$ alloys subjected to ten H–D cycles.

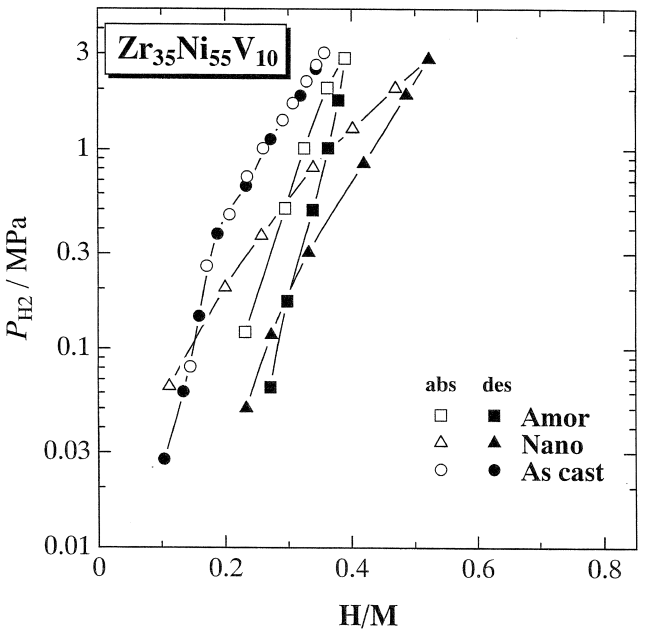

Fig. 7. *P–C–T* characteristics at 423 K of amorphous, nanocrystalline (crystallized at 973 K) and as-cast $Zr_{35}Ni_{55}V_{10}$ alloys subjected to ten H–D cycles.

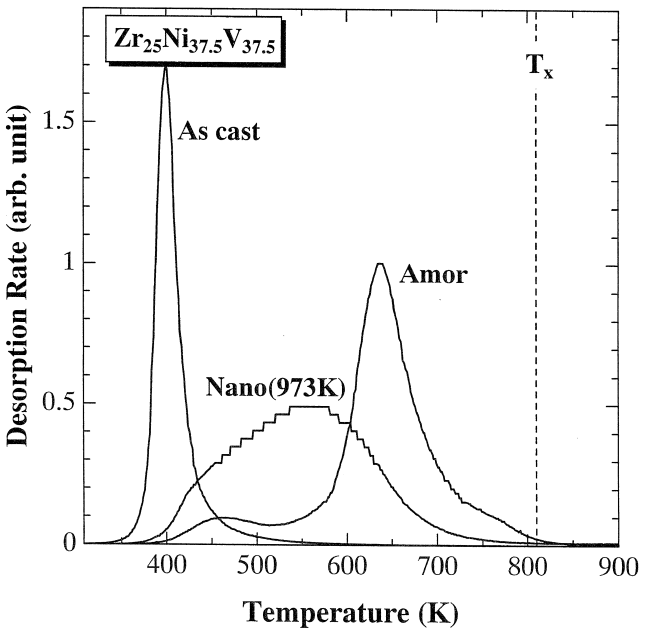

Fig. 8. TDS spectra of amorphous, nanocrystalline (crystallized at 973 K) and as-cast $Zr_{25}Ni_{37.5}V_{37.5}$ alloys loaded with the maximum amounts of hydrogen.

4. Summary and conclusions

Nanocrystalline Zr–Ni–V alloys near the equiatomic composition with C14 or C15 structure and a grain size of 5–10 nm can be obtained by crystallizing their amorphous phases at moderate temperatures. These nanocrystalline alloys exhibit hydrogen absorbency and H–D kinetics

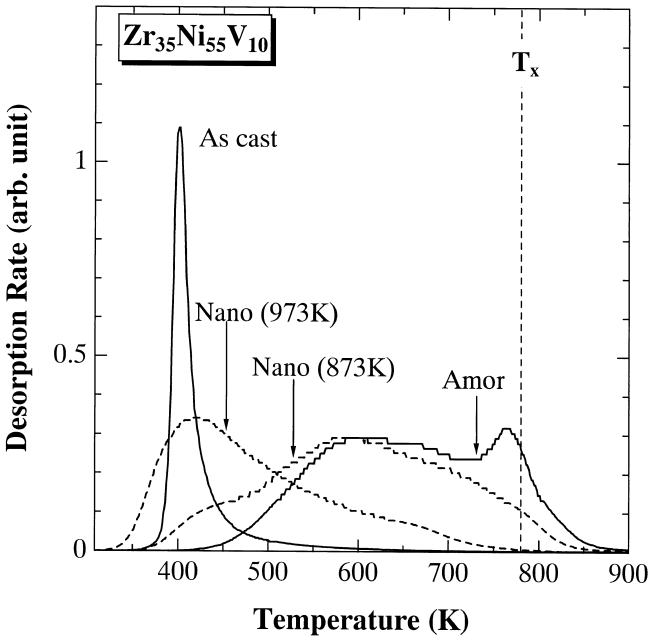

Fig. 9. TDS spectra of amorphous, nanocrystalline (crystallized at 873 and 973 K) and as-cast $Zr_{35}Ni_{55}V_{10}$ alloys loaded with the maximum amounts of hydrogen.

superior to those of the amorphous alloys. Their hydrogen absorbency is comparable or even higher than that of the as-cast alloys with equilibrium crystalline phases; however, their desorptive properties as revealed by TDS are poor in comparison with the latter. By optimizing the crystallization conditions, the desorptive properties may be much improved. For accomplishing the purpose, further studies by TEM techniques in particular are required to reveal the effects of crystallization conditions and H–D treatments on the microstructure of the nanocrystalline alloys.

Acknowledgements

This work is partly supported by the Grant-in-Aid for scientific research on priority areas A of new protium function from The Ministry of Education, Science, Sports and Culture of Japan (No. 10148105).

References

[1] H. Sawa, S. Wakao, Mater. Trans. J. Inst. Metals 31 (1990) 487.
[2] A. Züttel, D. Chartouni, K. Gross, M. Bächler, L. Schlapbach, J. Alloys Comp. 253 (1997) 587.
[3] D. Lupu, A.R. Biris, E. Indrea, A.S. Biris, G. Bele, L. Schlapbach, A. Züttel, J. Alloys Comp. 291 (1999) 289.
[4] K. Tanaka, Y. Kanda, M. Furuhashi, K. Saito, K. Kuroda, H. Saka, J. Alloys Comp. 293 (1999) 521.
[5] K. Tanaka, T. Araki, T. Abe, O. Yoshinari, J. Less-Common Metals 172 (1991) 928.
[6] L. Zaluski, A. Zaluska, P. Tessier, J.O. Ström-Olsen, R. Schulz, J. Alloys Comp. 227 (1995) 53.
[7] L. Zaluski, A. Zaluska, J.O. Ström-Olsen, J. Alloys Comp. 253–254 (1997) 74.
[8] A. Zaluska, L. Zaluski, J.O. Ström-Olsen, J. Alloys Comp. 288 (1999) 217.